Journal of The Electrochemical Society, **156** (8) D283-D286 (2009)
0013-4651/2009/156(8)/D283/4/$25.00 © The Electrochemical Society

Phosphorus Particle Composite Plating with Ni–P Alloy Matrix

Yosuke Suzuki,[a,*] Susumu Arai,[a,,z] Ikuo Shohji,[b] and Eiji Kobayashi[c]**

[a]*Faculty of Engineering, Shinshu University, Nagano 380-8553, Japan*
[b]*Faculty of Engineering, Gunma University, Gunma 376-8515, Japan*
[c]*Jintech Incorporated, Gunma 376-0011, Japan*

Ni–P alloy films containing phosphorus particles (called "Ni–P alloy composite films") were fabricated by electrodeposition and were subsequently subjected to heat-treatment. Their compositions and microstructures were characterized, and their friction properties were evaluated using a ball-on-plate method. Composite electroplating in the nickel sulfate and chloride bath containing phosphorus acid and micrometer-sized phosphorus particles resulted in the Ni–P alloy coating with enhanced deposit phosphorus content. The phosphorus content of the films increased with increasing phosphorus particle concentration in the composite plating baths, reaching a maximum value of 29.0 atom %. The phosphorus particles were homogeneously distributed in this Ni–29.0 atom % P alloy composite film. Heat-treatment converted the phases of the alloy composite films from an amorphous phase to stable crystalline phases, which are the same as those in the Ni–P binary alloy phase diagram. The friction coefficients of the Ni–P alloy films increased with increasing cycle number, whereas those of the Ni–P alloy composite films remained relatively constant. The alloy composite films had lower friction coefficients than the Ni–P alloy films both before and after heat-treatment. These results indicate that phosphorus particles are beneficial for maintaining a lower and stable friction coefficient during the ball-on-plate reciprocating friction test.
 [DOI: 10.1149/1.3142391]

Manuscript submitted December 12, 2008; revised manuscript received May 1, 2009. Published June 4, 2009.

Ni–P alloy plating has been extensively used in the industry because it confers good physical and chemical properties, including high hardness and high wear and corrosion resistances. Ni–P alloy films are conventionally fabricated by electroplating and electroless plating.[1-8] Most reports discuss alloy films with phosphorus contents less than 25 atom %, which have stable phases of Ni and Ni_3P according to the Ni–P binary phase diagram. However, the phase diagram indicates that $Ni_{12}P_5$ and other crystalline phases are stable when the phosphorus content of Ni–P alloys exceeds 25 atom %. Although some reports have discussed the microtexture of Ni–P alloy films with phosphorus contents of over 25 atom %,[6-9] the existence of $Ni_{12}P_5$ or other phosphorus-rich nickel–phosphorus compounds has never been reported.

Comparison of the microstructures and characteristics of Ni–P alloy films having phosphorus contents greater than 25 atom % with those of alloy films having phosphorus contents under 25 atom % is interesting from both academic and practical viewpoints. We initially fabricated Ni–P alloy films using a conventional electroplating method; however, the maximum phosphorus content that could be achieved by this method was less than 25 atom %.

In the present study, to fabricate Ni–P alloy films with phosphorus contents greater than 25 atom %, we used a composite plating method in which phosphorus particles are incorporated into Ni–P alloy films (Ni–P alloy composite plating). We also analyzed the microstructures of the composite films and evaluated their friction properties both before and after heat-treatment.

Experimental

A Ni–P alloy plating bath (1 M $NiSO_4 \cdot 6H_2O$ + 0.2 M $NiCl_2 \cdot 6H_2O$ + 0.5 M H_3BO_3 + 1 M H_3PO_3 + 0.5 M $C_6H_5Na_3O_7$) was used as the base bath. A Ni–P alloy phosphorus particle composite plating bath was prepared by adding amorphous red phosphorus particles (Wako Pure Chemical Industries, Ltd.) to this bath. The phosphorus particles were milled to diameters of 2–3 μm using a zirconia pot and zirconia balls. An electrolytic cell (model I, Yamamoto-Ms Co., Ltd.) with internal dimensions of 65 × 65 × 95 mm was employed for electrodeposition. The volume of the plating bath was 250 cm^3. Pure copper plates (C1020P) and stainless steel plates (SUS304), both having exposed surface areas of 10 cm^2 (3 × 3.3 cm^2), were used as substrates. A pure nickel plate was used as the anode. Plating was performed at 25°C with aeration under galvanostatic conditions (current density = 5 A dm^{-2} and electric charge = 600 C). The compositions of the deposited films were measured using an inductively coupled plasma (ICP; ICPS-7500, Shimadzu Seisakusho Co.). The deposited films were heat-treated in vacuum at 400°C for 1 h using an IR heating furnace (minilamp annealer; MILA-3000, ULVAC-RIKO Inc.). Their phase structures were analyzed using an X-ray diffractometer (XRD-6000, Shimadzu Seisakusho Co.). Their surface morphologies and cross-sectional textures were observed using a field-emission scanning electron microscope (JSM-7000F, JEOL). Mapping analysis of the cross sections of the deposits was performed by electron-probe X-ray microanalysis (EPMA; EPMA-1610, Shimadzu Seisakusho Co.). A cross-section polisher (SM-09010, JEOL) was used to prepare cross-sectional samples for observation. Hardness testing of the deposited films was performed using a micro-Vickers hardness tester (DUH-201, Shimadzu Seisakusho Co.). Their friction properties were measured using a ball-on-plate reciprocating friction tester (MMS-2419, Nissho Denki Co.), and a 6.1 mm diameter alumina ball (Hv = 1500) was used as the counter surface. The reciprocating friction stroke was 8 mm, and the tests were conducted under a normal load of 2 N. The sliding speed was 0.5 mm s^{-1} and the number of cycles was 50. All measurements were performed under ambient conditions without any lubricants.

Results and Discussion

Figure 1 shows the relationship between the concentration of phosphorus particles in the plating bath and the phosphorus content in the electrodeposited films. In most reports, the phosphorus contents of Ni–P alloy films were measured using energy-dispersive spectroscopy and EPMA.[5-9] In this study, the phosphorus contents of fabricated films were measured by ICP to evaluate the average phosphorus content of the whole fabricated films. The Ni–P alloy film electrodeposited from the bath without phosphorus particles contains 15.9 atom % phosphorus. The phosphorus content of the deposited films increased as the phosphorus particle concentration increased, reaching a maximum value of 29.0 atom %. Homogeneous composite films could not be fabricated when the phosphorus particle concentration in the plating bath exceeded 10 g dm^{-3}.

Figure 2a and b shows scanning electron microscopy (SEM) images of the surfaces of the Ni–15.9 atom % P alloy film and the Ni–29.0 atom % P alloy composite film, respectively. The Ni–15.9 atom % P alloy film is very flat (Fig. 2a). By contrast, the surface of

* Electrochemical Society Student Member.
** Electrochemical Society Active Member.
z E-mail: araisun@shinshu-u.ac.jp

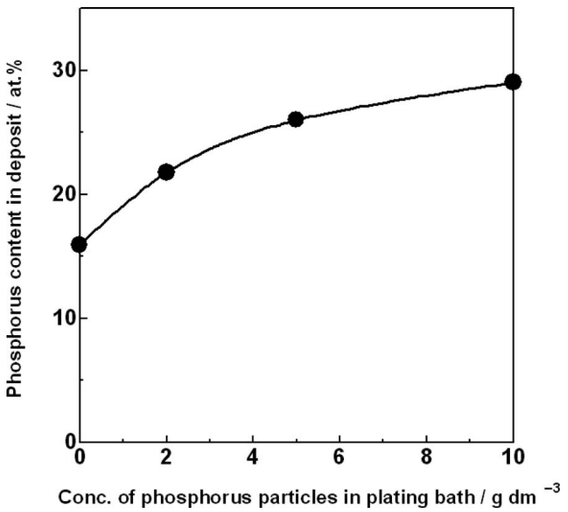

Figure 1. Relationship between phosphorus particle concentration in the plating bath and phosphorus content in the electrodeposited film.

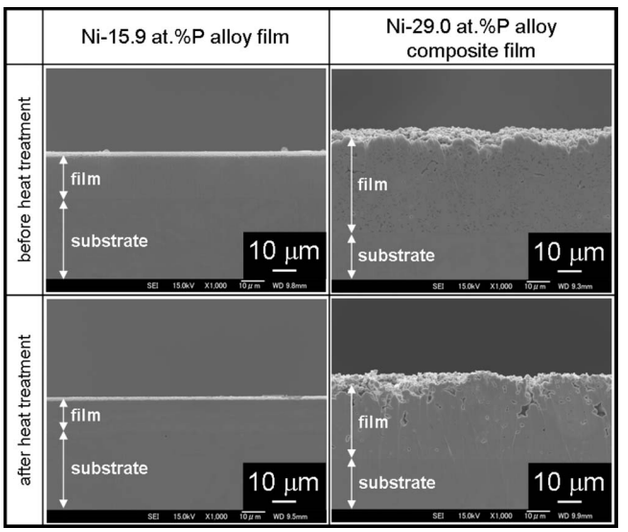

Figure 3. Cross sections of the Ni–15.9 atom % P alloy film and the Ni–29.0 atom % P alloy composite film before and after heat-treatment.

the Ni–29.0 atom % P alloy composite film is relatively rough, but the phosphorus particles are homogeneously distributed on its surface (Fig. 2b).

Figure 3 shows cross sections of the Ni–15.9 atom % P alloy film and the Ni–29.0 atom % P alloy composite film before and after heat-treatment. The Ni–15.9 atom % P alloy film is very dense and undergoes no major changes during heat-treatment. By contrast, the Ni–29.0 atom % P alloy composite film contains some voids both before and after heat-treatment. Figure 3 also shows that the thicknesses of the Ni–15.9 atom % P alloy film and the Ni–29.0 atom % P alloy composite film are reduced by heat-treatment.

Figure 4 shows the mapping analysis of a cross section of the Ni–29.0 atom % P alloy composite film before and after heat-treatment. Before heat-treatment, phosphorus particles are homogeneously distributed throughout the Ni–P alloy matrix. After heat-treatment, however, phosphorus and nickel are homogeneously distributed in the film and no phosphorus particles are observable. This indicates that heat-treatment causes interdiffusion between phosphorus particles and the Ni–P alloy matrix, causing the phosphorus particles to disappear and a homogeneous Ni–P phase to form.

Figure 5 shows X-ray diffraction (XRD) patterns of the Ni–15.9 atom % P alloy film and the Ni–29.0 atom % P alloy composite film before and after heat-treatment. Before heat-treatment, both films have broad peaks that are assigned to nickel. After heat-treatment, the nickel peaks of the Ni–15.9 atom % P alloy film become narrower and peaks assigned to Ni_3P also appear in the XRD patterns. By contrast, only peaks assigned to $Ni_{12}P_5$ are visible in the XRD patterns of the Ni–29.0 atom % P alloy composite films after heat-treatment. These results indicate that the films are transformed to the stable crystalline phase by heat-treatment, in agreement with the Ni–P binary alloy phase diagram (Fig. 6).

Figure 7 shows the hardnesses of the Ni–15.9 atom % P alloy film and the Ni–29.0 atom % P alloy composite film before and after heat-treatment. The hardnesses of the Ni–15.9 atom % P alloy film and the Ni–29.0 atom % P alloy composite film increased by heat-treatment. The increased hardness of the Ni–15.9 atom % P alloy film is attributed to the precipitation of the Ni_3P phase in that film. These results agree with those reported by Hou et al.[5] and Bai and Hu.[9] The increased hardness of the Ni–29.0 atom % P alloy composite film is attributed to a difference between the hardness of the composite film with phosphorus particles and that of $Ni_{12}P_5$. Both before and after heat-treatment, the hardnesses of the Ni–29.0 atom % P alloy composite films were lower than that of the Ni–15.9 atom % P alloy film. This reduction in hardness is conjectured by the existence of voids in the Ni–29.0 atom % P alloy composite film. Precipitation hardening did not occur during heat-treatment because the Ni–29.0 atom % P alloy composite film has a single phase after heat-treatment.

Figure 8 shows the relationship between the cycle number and the friction coefficient of the Ni–15.9 atom % P alloy film and the

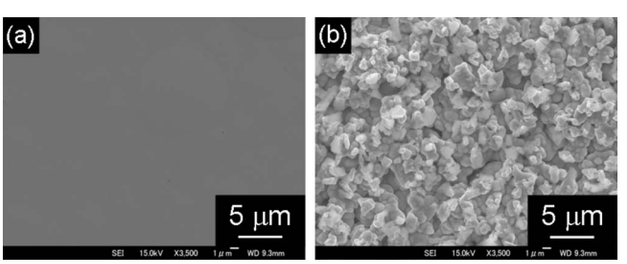

Figure 2. SEM images of the surfaces of (a) Ni–15.9 atom % P alloy film and (b) Ni–29.0 atom % P alloy composite film.

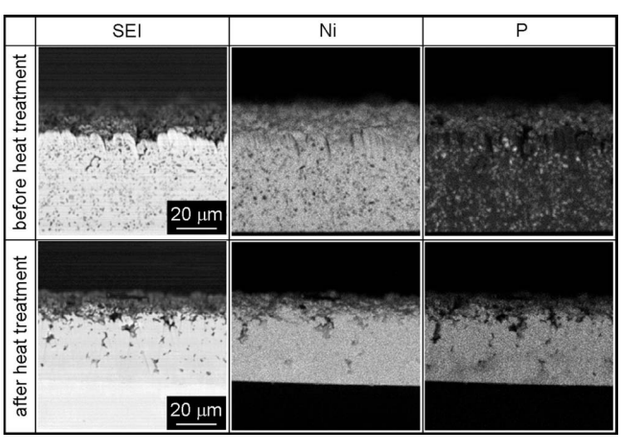

Figure 4. Mapping analysis of a cross section of the Ni–29.0 atom % P alloy composite film before and after heat-treatment.

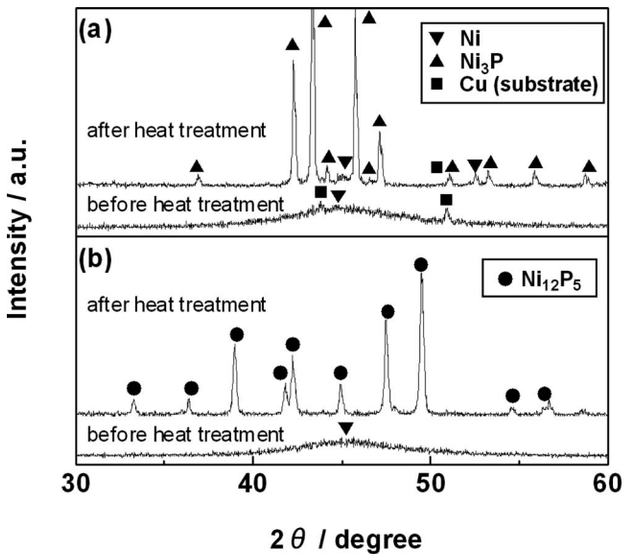

Figure 5. XRD patterns of (a) the Ni–15.9 atom % P alloy film and (b) the Ni–29.0 atom % P alloy composite film before and after heat-treatment.

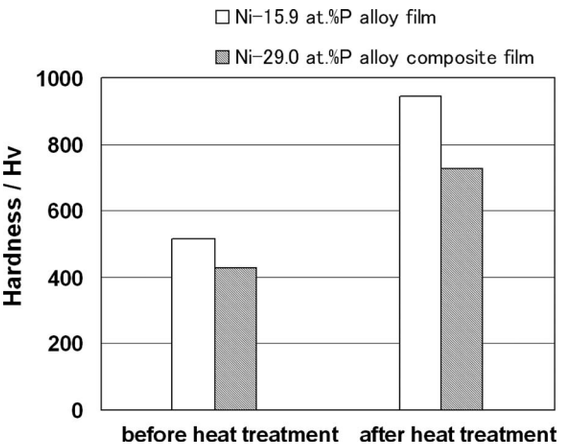

Figure 7. Hardnesses of the Ni–15.9 atom % P alloy film and the Ni–29.0 atom % P alloy composite film before and after heat-treatment.

Ni–29.0 atom % P alloy composite film before heat-treatment. The friction coefficient of the Ni–15.9 atom % P alloy film increases with increasing cycle number. By contrast, the friction coefficient of the Ni–29.0 atom % P alloy composite film remains nearly constant with increasing cycle number. Thus, the phosphorus particles may act as a lubricant. Sedlaček et al. reported that the friction coefficient was lower with the increase in surface roughness under no lubricant.[10] Figures 2 and 3 show that the Ni–29.0 atom % P alloy composite film has a rougher surface than the Ni–15.9 atom % P alloy film. Therefore, a decrease in the friction coefficient of the Ni–29.0 atom % P alloy composite film may be attributed to the difference in the surface roughness of that film.

Figure 9 shows the relationship between the cycle number and the friction coefficient of the Ni–15.9 atom % P alloy film and the Ni–29.0 atom % P alloy composite film after heat-treatment. Before heat-treatment, the friction coefficient of the Ni–15.9 atom % P alloy film tends to increase with increasing cycle number, while that of the Ni–29.0 atom % P alloy composite film remains nearly constant with increasing cycle number. These results may be attributed to the lower friction coefficient of $Ni_{12}P_5$ and the surface roughness of the film.

Figure 10 shows SEM images of worn surfaces of the Ni–15.9 atom % P alloy film and the Ni–29.0 atom % P alloy composite film before heat-treatment. The entire surface of the worn area of the Ni–15.9 atom % P alloy film is damaged, whereas the Ni–29.0 atom % P alloy composite film was damaged only on convex sections of its surface. Phosphorus particles are observed on the worn surface of the Ni–29.0 atom % P alloy composite film. These results are related to the lower friction coefficient of the Ni–29.0 atom % P alloy composite film in Fig. 8.

Figure 11 shows SEM images of worn surfaces of the Ni–15.9 atom % P alloy film and the Ni–29.0 atom % P alloy composite film after heat-treatment. As with films before heat-treatment, the entire surface of the worn area of the Ni–15.9 atom % P alloy film was damaged, whereas the Ni–29.0 atom % P alloy composite film was

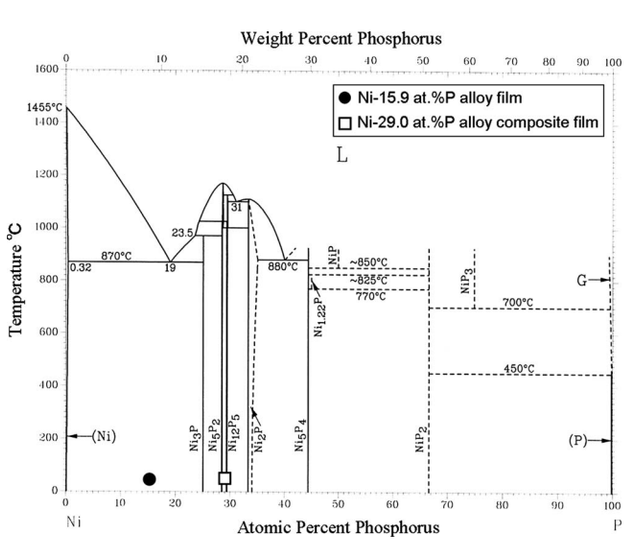

Figure 6. Ni–P binary alloy phase diagram.

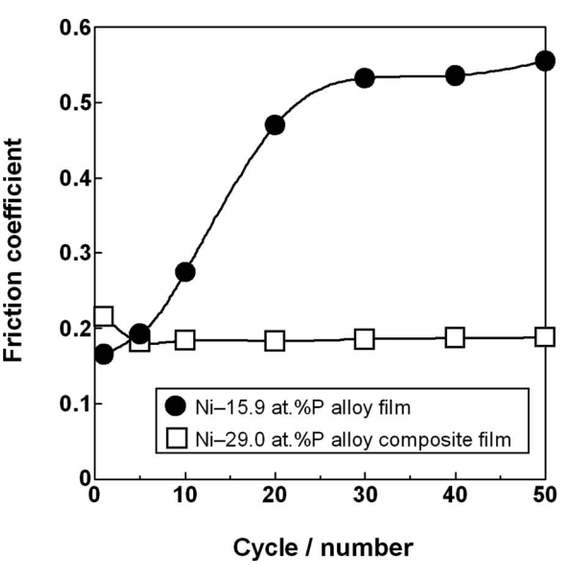

Figure 8. Relationship between cycle number and friction coefficients of the Ni–15.9 atom % P alloy film and the Ni–29.0 atom % P alloy composite film before heat-treatment.

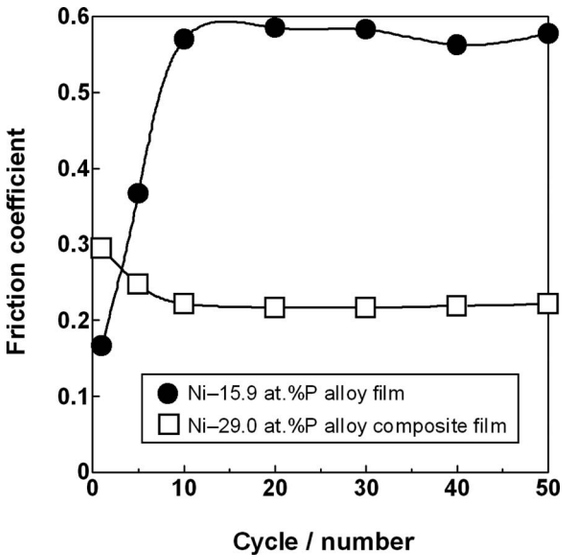

Figure 9. Relationship between cycle number and friction coefficients of the Ni–15.9 atom % P alloy film and the Ni–29.0 atom % P alloy composite film after heat-treatment.

damaged only on convex sections of its surface. These results are related to the lower friction coefficient of the Ni–29.0 atom % P alloy composite film in Fig. 9.

Conclusions

Ni–P alloy composite plating was investigated. The main conclusions are as follows.

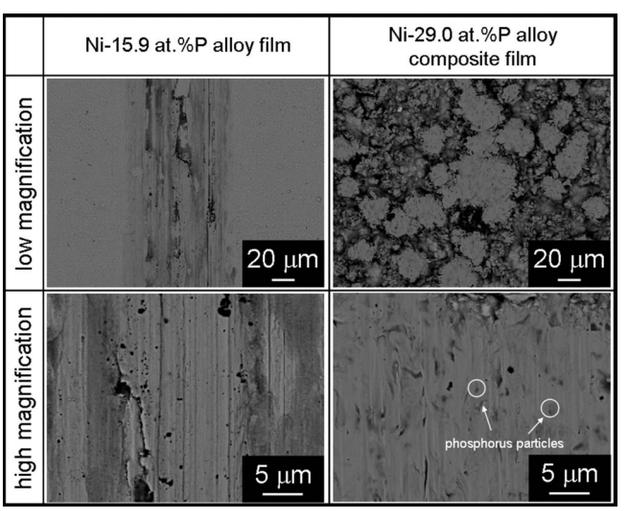

Figure 10. SEM images of worn surfaces of the Ni–15.9 atom % P alloy film and the Ni–29.0 atom % P alloy composite film before heat-treatment.

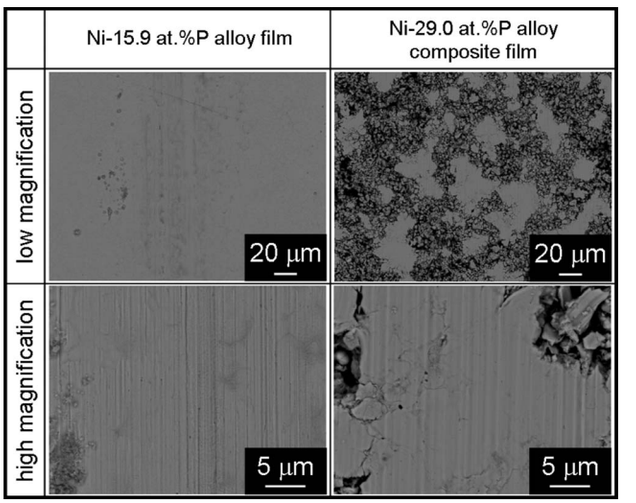

Figure 11. SEM images of worn surfaces of the Ni–15.9 atom % P alloy film and the Ni–29.0 atom % P alloy composite film after heat-treatment.

1. The phosphorus content in the deposits increased with increasing phosphorus particle concentration in the bath, reaching a maximum value of 29.0 atom %.
2. The phosphorus particles were distributed relatively uniformly in the Ni–P alloy film.
3. When the Ni–29.0 atom % P composite film was heat-treated, the phase of the Ni–29.0 atom % P composite film was converted to the stable crystalline phase, in agreement with the Ni–P binary alloy phase diagram.
4. Both before and after heat-treatment, the hardness of the Ni–29.0 atom % P alloy composite film was lower than that of the Ni–15.9 atom % P alloy film.
5. The hardness of the film composed of Ni and Ni_3P was larger than that of the film mainly composed of $Ni_{12}P_5$.
6. Both before and after heat-treatment, the friction coefficient of the Ni–29.0 atom % P alloy composite film was lower than that of the Ni–15.9 atom % P alloy film.

Shinshu University assisted in meeting the publication costs of this article.

References

1. H. Ashassi-Sorkhabi and S. H. Rafizadeh, *Surf. Coat. Technol.*, **176**, 318 (2004).
2. M. H. Seo, J. S. Kim, W. S. Hwang, D. J. Kim, S. S. Hwang, and B. S. Chun, *Surf. Coat. Technol.*, **176**, 135 (2004).
3. A. P. Ordine, S. L. Díaz, I. C. P. Margarit, O. E. Barcia, and O. R. Mattos, *Electrochim. Acta*, **51**, 1480 (2006).
4. I. Baskaran, T. S. N. Sankara Narayanan, and A. Stephen, *Mater. Chem. Phys.*, **99**, 117 (2006).
5. K. H. Hou, M. C. Jeng, and M. D. Jeng, *J. Alloys Compd.*, **437**, 289 (2007).
6. E. Bredael, B. Blanpain, J. P. Celis, and J. R. Roos, *J. Electrochem. Soc.*, **141**, 294 (1994).
7. C. C. Hu and A. Bai, *Mater. Chem. Phys.*, **77**, 215 (2002).
8. C. C. Hu and A. Bai, *Surf. Coat. Technol.*, **137**, 181 (2001).
9. A. Bai and C. C. Hu, *Mater. Chem. Phys.*, **79**, 49 (2003).
10. M. Sedlaček, B. Podgornik, and J. Vižintin, *Wear*, **266**, 482 (2009).